Mon. Not. R. Astron. Soc. **322**, 356–360 (2001)

Fine structure in the inner dust shell of IRC+10216 from lunar occultation observations at 2.2 μm

T. Chandrasekhar★ and Soumen Mondal

Physical Research Laboratory, Ahmedabad 380009, India

Accepted 2000 October 9. Received 2000 October 9; in original form 2000 May 2

ABSTRACT

Lunar occultation observations of the inner dust shell surrounding the carbon-rich long-period variable IRC+10216 obtained in the near-infrared *K* band have yielded a one-dimensional scan across the source (at position angle 304°) with a high angular resolution of 1 milliarcsec. Analysis of the occultation light curve shows significant departures from a spherically symmetric uniform disc model, indicating that the dust shell of IRC+10216 is extremely clumpy. Apart from a dominant component A, at least three other components (B, C, D) are seen within the clumpy structure. Comparison with earlier speckle observations confirms that real spatial changes are taking place in the clumpy structure over time-scales of a few years.

Key words: occultations – Moon – stars: AGB and post-AGB – stars: individual: IRC+10216 – stars: mass-loss – infrared: stars.

1 INTRODUCTION

IRC+10216 (CW Leo) is a carbon-rich long-period variable with an unusually thick circumstellar dust shell embedded in a molecular envelope. Being one of the closest and brightest [at mid-infrared (IR) wavelengths] carbon-rich evolved stars on the asymptotic giant branch (AGB) of the Hertzsprung–Russell (HR) diagram it has been the focus of attention for numerous theoretical and observational investigations pertaining to the late phases of stellar evolution, mass-loss processes, formation of protoplanetary nebulae and chemical enrichment of the galaxy. About 50 molecular species have been detected in the circumstellar envelope of IRC+10216, making it one of the best examples of carbon-rich circumstellar chemistry.

IRC+10216 is an extreme carbon star of spectral type C 9.5 (Olofsson et al. 1982). Its distance estimates have ranged from 100 pc (Zuckerman, Dyck & Claussen 1986) to 290 pc (Herbig & Zappala 1970). Some recent estimates give a value of 120 pc (Loup et al. 1993). More recently, Crosas & Menten (1997) have used submillimetre observations to constrain the distance to IRC+10216 to a value of 150 pc. We adopt this value for future discussions.

IRC+10216 is a long-period variable with a period which varies between 628 and 649 d (Jones et al. 1990, Le Bertre 1992). It is shedding mass with a terminal velocity of 15 km s^{-1} (Knapp 1985). Most mass-loss estimates give a value of 2×10^{-5} M$_{\odot}$ yr^{-1} (Mauron & Higgins 1999). The corresponding dust mass-loss rate is 1.0×10^{-7} M$_{\odot}$ yr^{-1} and the stellar effective temperature is ~2000 K (Skinner, Meixner & Bobrowsky 1998). The low effective temperature, long period and high mass-loss rate indicate an advanced stage of AGB evolution. The carbon-rich environment suggests the occurrence of several thermal pulses and consequent dredge-up events. The non-spherical appearance of the dust envelope [800 milliarcsec (mas) in NS and 600 mas in EW] also suggests that the star has entered a phase immediately before moving off the AGB (Weigelt et al. 1998).

High angular resolution studies of the central region of IRC+10216 where the radiation field is the strongest have had a long history since the pioneering lunar occultation observations by Toombs et al. (1972). Sutton et al. (1979), using the infrared spatial interferometer, observed the envelope structure of IRC+10216 at 11.2 μm on a spatial scale ranging between 0.5 and 1 arcsec. They did not see significant departures from circular symmetry. They reported a maximum ellipticity of <1.1 and an optical depth at 11 μm of 0.5. Later again at the same wavelength Danchi et al. (1994) studied the spatial distribution of dust surrounding IRC+10216 at several epochs. They found that the visibility curves changed with the luminosity phase of the star and suggested formation of new dust during minimum luminosity of the star. Using visibility curves calculated from spherically symmetric three-dimensional (3D) radiative transfer models of dust they derived from their measurements the inner radius of the dust shell to be 70 mas at minimum and an optical depth at 11 μm of 1.44. More recently, detailed radiative transfer calculations using spectroscopic and visibility data have been carried out by Gronewegen et al. (1997), while consistent time-dependent models of circumstellar dust formation around long-period variables have been studied by Fleischer, Gauger & Sedimayr

★ E-mail: chandra@prl.ernet.in

(1992). A general result of these models is the formation of discrete dust layers with time-varying intensity distributions.

Le Bertre (1987) has modelled photometric data between 0.5 and 20 μm, obtained during minimum phase in a radiative transfer model consisting of a central star surrounded by a circumstellar dust shell. A dust opacity law of $\lambda^{-1.3}$ reproduces the general spectrum characteristics well. The model obtained with a $\lambda^{-1.3}$ law gives intensity profiles that are consistent with infrared spatial measurements. According to this model scattering by dust grains is important at 0.6 μm but becomes negligible at 2.2 μm.

Using early speckle interferometric techniques at 2.2 and 10.3 μm, Dyck et al. (1987) found the source to be elongated at a position angle of 20° at 2.2 μm, but nearly circular at 10.3 μm. They suggested a model consisting of a thick equatorial disc tilted to the line of sight by ~50°. The polarimetric, coronagraphic images of IRC+10216 in *J*, *H* and *K* by Kastner & Weintraub (1994) also showed strong evidence of large-scale asymmetry within the circumstellar envelope. More recently, Haniff & Buscher (1998), using speckle observations at 2.2 and 3.4 μm, found the source to be strongly asymmetric and hence incompatible with spherical models of radiatively heated dust. They pointed out that minor modifications to spherical models to include scattering component are inadequate to explain high angular resolution observations of the inner zone of IRC+10216.

In recent years, near-infrared speckle interferometry has revealed the presence of bright blobs within the inner dust shell of IRC+10216 located within 400 mas of the centre (Haniff & Buscher 1998; Weigelt et al. 1998). The fragmentation of shell structure is interpreted as evidence of inhomogeneous mass loss. It appears that IRC+10216 is poised at a very interesting and advanced state of its AGB evolution before turning into a protoplanetary nebula.

In this paper we present a rare recent *K*-band lunar occultation observation of IRC+10216 which has potentially a one-dimensional (1D) spatial resolution of ~1 mas. Fine structures in the occultation light curve are analysed to obtain the relative positions of the secondary sources in the inner dust shell surrounding IRC+10216.

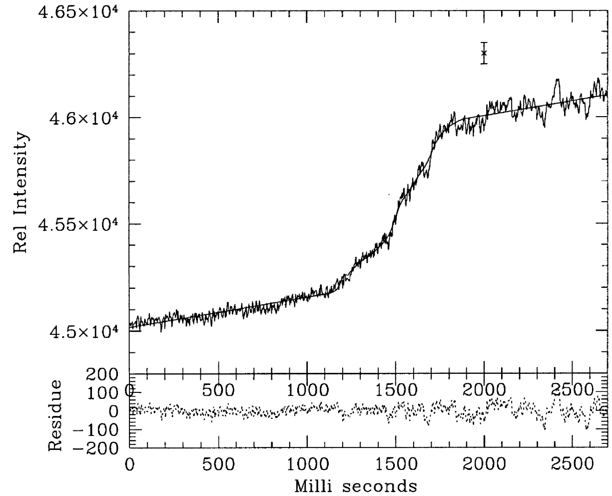

Figure 1. Lunar occultation light curve of IRC+10216 in the *K* band and the best model fit to the curve. The residual (data−model) is shown on the same scale at the bottom. The error bars show the extent of scintillation noise after emergence.

Table 1. Circumstances of lunar occultation event of IRC+10216 at Gurushikhar Observatory.

Date	1998 Dec. 08
Event time (UT)	$19^h 16^m 36\overset{s}{.}6 \pm 0\overset{s}{.}5$
Position angle (NESW)	304°
Contact angle	203°
Predicted velocity component of Moon in direction of occultation (km s^{-1})	−0.7728
Predicted angular velocity component in direction of occultation (arcsec s^{-1})	−0.4156
Lunar phase (days after new Moon)	19.57
Photometric variability phase	0.67
Data sampling rate	1 ms
Photometer diaphragm on the sky (arcsec)	26
Altitude of event	26°
Sky condition	Photometric

2 THE OBSERVATIONS

A unique opportunity for observing lunar occultation of IRC+10216 occurred on 1998 December 8 at Gurushikhar Observatory, Mt Abu, India (latitude: 24° 39′ 8″.8 N, longitude: 72° 46′47″.47 E, altitude: 1680 m). A single-element InSb detector dewar operating in the broad *K* band ($\lambda = 2.2\,\mu$m, $\Delta\lambda \simeq 0.4\,\mu$m) was attached to the 1.2-m telescope and used to successfully record the reappearance lunar occultation event of IRC+10216. Details of the instrument used for lunar occultation observations can be found elsewhere (Ashok et al. 1994; Chandrasekhar 1999). Basically the high-speed IR photometer records the IR signal at a sampling rate of 1 ms without chopping during the event. The relatively large photometer diaphragm of 26 arcsec was used as this was a reappearance event. An unocculted source was tracked until about 5 min before the event and then the telescope was switched precisely to the position of the dark lunar limb at which emergence was to occur. Before the event the limiting noise is sky noise which is over ridden by scintillation noise once the star emerges. This can be clearly seen in Fig. 1. The rising slope seen in the light curve is caused by the increasing sky background within the diaphragm as the dark lunar limb recedes out; it is modelled as a simple linear addition to the star signal in the analysis. Immediately after the event the instrument time response is recorded with a fast IR light emitting diode (LED) and used later in the analysis.

The circumstances of the event are listed in Table 1. Photometry of the source in the *K* band resulted in a value $m_k = 2.06 \pm 0.07$. The photometric variability phase relative to Weigelt et al. (1998) on this day was 0.67.

3 ANALYSIS

The conventional method of analysis of lunar occultation light curves is to perform a multiparameter fit to the photometric recording following the method of Nather & McCants 1970. The parameters involved in the non-linear least-squares (NLS) method are five in number: (i) geometric time of occultation; (ii) star signal counts; (iii) background counts; (iv) velocity component of the Moon in the direction of occultation; and (v) the uniform disc angular diameter. The point source Fresnel diffraction pattern modulated by the finite spectral bandwidth of the system, the finite telescope aperture and the instrumental time response and by the finite angular size of the source are used to fit the data. In the case of IRC+10216, the source is so extended that diffraction effects are negligible. The conventional non-linear least-squares analysis for the occultation data yields a uniformly illuminated disc size of 295 ± 5 mas.

We have used a model-independent algorithm (MIA) introduced by Richichi (1989) to probe the structure of the dust envelope. MIA is a composite algorithm which makes use of the NLS method and Lucy's deconvolution algorithm wherein a guess profile, usually the uniform disc profile is iteratively modified to obtain the best fit to the data. Averaging effects arising from the finite optical filter bandwidth and the telescope aperture have also been accurately taken into account.

The signal-to-noise ratio in the data is limited by the scintillation noise seen on immersion in the occultation light curve. In the present case in order to improve the signal-to-noise ratio data have been binned to produce an effective sampling rate of 3 ms. As the lunar angular velocity component in the direction of occultation is 0.4156 arcsec s^{-1} the sampling rate corresponds to ~1.2 mas. The angular resolution of about 1 mas achievable in the case of lunar occultation, one dimensionally only in the direction of occultation compares favourably with the best speckle resolutions of about 70 mas.

Fig. 1 shows the observed occultation light curve covering 2700 ms around the time of the event. The best fit to the light-curve based on the MIA is shown superposed on the light curve. The model curve has as inputs the uniform disc diameter of 295 mas derived from the non-linear least-squares approach along with the velocity component frozen to the predicted value of $-0.7728\ \mathrm{km\,s^{-1}}$. The derived one-dimensional brightness profile, which gives the best fit to the observed occultation light curve has a background component superposed on the modulations arising from the individual sources. In order to bring out the source structure the contribution of the uniform disc model has been removed. The resultant brightness profile is shown in Fig. 2. It can be seen that the source is highly structured. In addition to a dominant component that we call A there are at least three other components (B, C, D) within ±100 mas of the centre. It may be noted that the departure from a uniform disc model is both positive and negative, indicating the presence of sources and depletions. Furthermore, there are many fine structures located with respect to centre at −107, −15, +52, +69 and +103 mas.

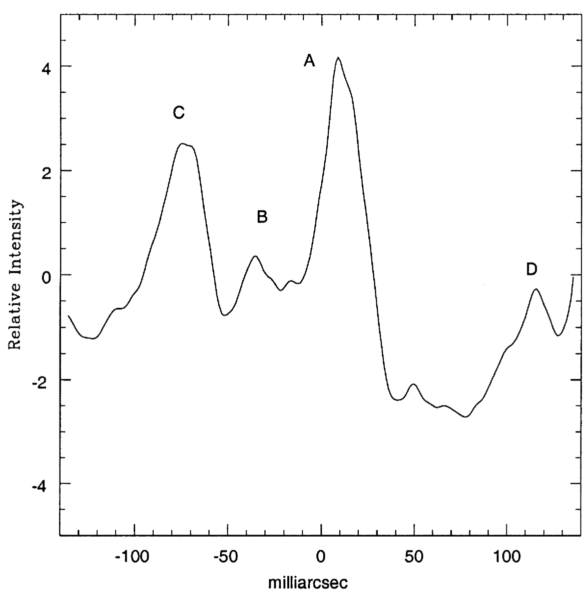

Figure 2. The best-fitting brightness profile of the source from which the contribution of a uniform disc profile has been subtracted. The main components A–D are identified

The relative positions of the components and their relative intensities with respect to A are listed in Table 2. The relative intensities are taken to be enhancements above the uniform disc level and may not be truly representative of the individual component intensities.

4 RESULTS AND DISCUSSION

The brightness profile in Fig. 2 is a high-resolution one-dimensional profile, along the position angle of the event, of the two-dimensional (2D) dust cloud of IRC+10216. Furthermore, a uniform brightness profile has been subtracted from it. It cannot be compared straightaway with the speckle images and intensity contours. In order to compare our observations with the speckle observations of Haniff & Buscher (1998) and Weigelt et al. (1998) it is necessary to project their 2D images on to the direction of our occultation. While making the comparison it needs to be noted that apart from the one-dimensional nature of lunar occultation observations, we are also limited by the relatively poorer angular resolution of speckle observations (~70 mas). Haniff & Buscher obtained several thousand short-exposure images of IRC+10216 using 2D array detectors in 1989 May (phase 0.34) and in 1997 March (phase 0.82) through narrow-band filters centred at 2.2 and 3.4 μm. While the different bandwidths used by different observers makes a detailed comparison of relative brightness distribution difficult it does not affect the relative positional measurements of the four components A, B, C, D with which we are primarily concerned. Operating at a diffraction-limited resolution of 0.1 arcsec they found considerable changes in the morphology of near-IR emission from 1989 to 1997. While in 1989 both *K*- and *L*-band emissions had a dominant single core, in 1997 four components were reported: the brightest (A) towards the south and the other three in relation to the bright component (A) were located at position angles 20° − 30° and 65° at separations of 230 mas (B), 210 mas (C) and 200 mas (D). The intensity of B is about 30 per cent of A at 2.2 μm.

Weigelt et al. (1998) using the K' filter (2.17 μm) at a spatial

Table 2. Relative positions and intensities of components in the derived brightness profile of IRC+10216.

Component	Location relative to centre of uniform disc profile (mas)	Projected angular separation from A (mas)	Rel. int.
A	+11	–	1.0
B	−34	45	0.046
C	−74	85	0.64
D	+117	106	0.053

Table 3. Comparison with speckle observations of IRC+10216.

Observation date	1996 April	1997 March	1998 Nov.	1998 Dec. 08 (this work)
Variability phase	0.15	0.82	0.61	0.67
Technique	Speckle	Speckle	Speckle	LO
Angular resolution (mas)	76	100	76	1 (1D along PA 304°)
Separation AB (mas)				
(PA of B: 20°)	203	230	265	186
Separation AC (mas)				
(PA of C: 339°)	137	210	178	104
Separation AD (mas)				
(PA of D: 65°)	136	200	200	206
Projected separation along PA 304° (mas)				
AB	45	54	64	45
AC	112	188	148	85
AD	58	104	103	106
References	2	1	3	This work

(1) Haniff et al. (1998); (2) Weigelt et al. (1998); (3) Osterbart et al. (2000).

resolution of 76 mas, find the dust shell to be extremely clumpy, from their speckle observations of 1996 April (variability phase 0.15). In addition to a dominant central component (A) they identify three bright knots relative to A at position angles 21°, 339° and 59° at separations of 203 mas (B), 137 mas (C) and 136 mas (D). From the asymmetry of the dominant component they suggest two additional components (E and F), not fully resolved at separations from A of less than 100 mas.

The position angles of E and F are 122° and 200°, respectively, relative to A. Objects A–F are located inside a larger symmetric nebulosity which at the 2 per cent intensity level extends 800 mas in NS and 600 mas in EW. They also remark on the considerable brightness of B (~5 per cent of the total flux).

In a recent paper (Osterbart et al. 2000) these authors remark that the separation between the brightest components A and B has increased from 191 mas in 1995 to 265 mas in 1998. They derive a uniform angular expansion velocity of 23 mas yr^{-1} and for their assumed distance to the source of 130 pc, a motion of 14 km s^{-1} in the plane of the sky. At the same time they find component B to be fading, while C and D are becoming brighter. They also suggest the position of central star to be at or near the position of component B and not A. They find the observed charges to be consistent with an enhanced mass loss since 1997.

Considering the position angle of our occultation (304°) with respect to the position angles of sources A–D in Weigelt et al. (1998), in our reappearance event, first source C will be uncovered, then B, A and D. It may be pointed out that in the case of lunar occultation, while we are constrained to one dimension (along the direction of occultation), the projected separation between different components is obtained with high precision (±1 mas). In Table 3 we have compared the speckle interferometric observations with our work. Here we have listed along with our values the position angles and actual separation in milliarcsecs of sources B–D from the dominant component for the three cases of Haniff & Buscher (1998), Weigelt et al. (1998) and Osterbart et al. (2000). Although these observations are separated by a few years the position angles of the different components remain approximately the same but the actual separations have changed. Using the projection angles of components B–D relative to A we have also derived the expected actual separations AB, AC and AD for our measured projected separations. There is good agreement for AD. Our values for AB and AC are less than those obtained from speckle measurements. We have also obtained the projected separations for the speckle observations along the direction of occultation (PA 304°) to compare them with our values. It can be seen that while for B and D components the agreement between occultation observations and speckle is good for component C there appears to be a discrepancy. We further note that for component C we have obtained a large relative intensity value, over 60 per cent that of A. As can be seen from the speckle observations of 1998 November (Osterbart et al. 2000, fig. 1e) this arises from integration nearly along the direction CB in case of our one-dimensional lunar occultation brightness profile. There is substantial contribution to the signal at C from the neighbourhood of B, which could explain the large peak value.

Table 4. Length and time-scales of components.

	Derived angular separation (mas)	Linear separation ($\times 10^{14}$ km)	R/R_*	t (yr)
AB	186	4.19	8.38	9.3
AC	104	2.34	4.68	5.2
AD	206	4.64	9.28	10.3

As the occultation observation has a much higher angular resolution in one dimension compared with speckle work it is possible to refine the speckle results further by deriving 1D profile along occultation direction and comparing it with the observed occultation brightness profile.

According to Haniff & Buscher (1998) the high angular resolution data in the optical and infrared from 1997 can be explained by a geometric model with dominant bipolar axis along PA 5° and a half-opening angle of 20° to the line of sight. They interpret the 2.2 and 3.4 μm structures as additional components of thermal emission from clumps of dust that happen to lie closest to the central star in a plane perpendicular to the bipolar axis. The inclination of the torus permits a direct view of the inner envelope. However, at the present time it cannot be completely ruled out that the structures seen are not local density enhancements or sites of additional heating.

In Table 4 we have calculated, using the assumed distance to the source of 150 pc and a stellar radius of the underlying star of 5×10^{13} cm (Weigelt et al. 1998), the location of the structures in terms of stellar radius. A terminal velocity of 15 km s^{-1} at the distance to IRC+10216 corresponds to an expansion rate of 20 mas yr^{-1}. If we assume that components B–D have separated and moved away from A then the time-scales of expansion at this rate are 5–10 yr. This seems consistent with the observations of Haniff & Buscher (1998) that in 1989 they saw only a single dominant component. One could speculate on whether components B and D are part of a single event of dust ejection ~10 yr ago and whether C was subsequently ejected from A. The difference between the two events is ~3 periods of stellar variability.

It may be noted here that we have assumed the expansion to originate at or near A, while Osterbart et al. (2000) in their analysis favour a position at or near B as the position of the central star. A recent lunar occultation observation of IRC+10216 at a wavelength of 10 μm (Stecklum, Kaufl & Richichi 1999) has revealed the presence of three symmetric rings at larger radial distances of 210, 368 and 525 mas from the dominant source. These could have been ejected 10.5, 18.4 and 26.3 yr earlier. They suggest a time period between ejection of ~7.8 yr or 4.5 periods. It is, however, clear that every minima does not give rise to an ejection event. Close monitoring of IRC+10216 at high angular resolution in the near infrared in future could be very valuable in tracing the evolution of rapidly changing the dust structures around the star as it moves towards its protoplanetary phase.

5 CONCLUSIONS

Lunar occultation observations in the *K* band of IRC+10216 at a photometric phase of 0.67 have resulted in a one-dimensional high angular resolution profile of the inner dust shell regions of the source. The source brightness profile is found to be highly structured; it departs significantly from a uniform disc profile. Apart from a dominant component A it has been possible to identify from the occultation light curve at least three other components B–D seen by earlier speckle interferometric observations. There are fine structures at the level of milliarcseconds in the one-dimensional profile which can be modelled further using inputs from recent speckle observations.

ACKNOWLEDGMENTS

We thank the referee for his valuable comments. The authors are very grateful to Dr Andrea Richichi for detailed discussions on the analysis of occultation light curve of IRC+10216. They also would like to thank Dr Sam Ragland for the help in the use of the MIA program. Support for the work came from Department of Space, Government of India.

REFERENCES

Ashok N. M., Chandrasekhar T., Sam Ragland Bhatt H. C., 1994, Exp. Astron, 4, 177
Chandrasekhar T., 1999, Bull. Astron. Soc. India, 27, 43
Crosas M., Menten K. M., 1997, ApJ, 483, 913
Danchi W. C., Bester M., Degiacomi C. G., Greenhill L. J., Townes C. H., 1994, AJ, 107, 1469
Dyck H. M., Zuckerman B., Howell R. R., Beckwith S., 1987, PASP, 99, 99
Fleischer A. J., Gauger A., Sedimayr E., 1992, A&A, 266, 321
Gronewegm M. A. T., Van der Veen W.E.C.J., Lefloch B., Omont A., 1997, A&A, 322, L21
Haniff C. A., Buscher D. F., 1998, A&A, 334, L5
Herbig G. H., Zappala R. R., 1970, ApJ, 162, L15
Jones T. J., Bryja C. O., Gehrz R. D., Harrison T. E., Johnson J. J., Klebe D. I., Lawrence G. F., 1990, ApJS, 74, 785
Kastner J. H., Weintraub D. A., 1994, ApJ, 434, 719
Knapp G. R., 1985, ApJ, 293, 273
Le Bertre ., 1987, A&A, 176, 107
Le Bertre T., 1992, A&AS, 94, 377
Loup C., Forveille T., Omont A., Paul J. F., 1993, A&AS, 99, 291
Mauron N., Huggins P. J., 1999, AA, 349, 203
Nather R. F., McCants N. M., 1970, AJ, 75, 963
Oloffsson H., Johansson L. E. B., Hjalmarsson Aå., Nguyen-Quarg-Rieu ?., 1982, A&A, 107, 128
Osterbart R., Balega Y. Y., Blocker T., Men'shchikov A. B., Weigelt G., 2000, A&A, 357, 169
Richichi A., 1989, A&A, 226, 366
Skinner J., Meixner M., Bobrowsky M., 1998, MNRAS, 300, L29
Stecklum B., Kaufl H. V., Richichi A., 1999, Messenger, 95, 25
Sutton E. C., Betz A. L., Storey J. W. V., Spears D. L., 1979, ApJ, 230, L105
Toombs R. T., Becklin E. E., Frogel J. A., Law S. K., Porter F. C., Westphal J. A., 1972, ApJ, 173, L71
Weigelt G., Balega Y., Blocker T., Fleischer A. J., Osterbart R., Winters J. M., 1998, AA, 333, L51
Zuckerman B., Dyck H. M., Claussen M. J., 1986, ApJ, 304, 401

This paper has been typeset from a TEX/LATEX file prepared by the author.